

# Control of Grid-connected Inverter using Carrier Modulation

**Quang-Tho Tran**

Faculty of Electrical and Electronics Engineering, HCMC University of Technology and Education, Vietnam

thotq@hcmute.edu.vn (corresponding author)

Received: 10 May 2024 | Revised: 28 May 2024 | Accepted: 30 May 2024

Licensed under a CC-BY 4.0 license | Copyright (c) by the authors | DOI: <https://doi.org/10.48084/etasr.7789>

## ABSTRACT

Multilevel inverters are becoming prevalent due to their remarkable attributes, including their ability to withstand high voltage shocks and accommodate high capacity. As a result, they find extensive applications in grid-connected inverter systems utilizing photovoltaic (PV) panels and electric drive systems for electric motors. However, their power quality is heavily reliant on current controls and inverter modulation techniques. Conventional modulation methods typically employ fixed frequency carriers for inverter modulation, lacking inherent control signal information. In response to this challenge, this study proposes a novel modulation method for grid-connected multilevel inverters utilizing frequency and phase-modulated carriers. The study findings demonstrate the effectiveness of the proposed approach in the nominal operation, showcasing a reduction in Total Harmonic Distortion (THD) by 15.92% and a 48.5% decrease in the highest individual harmonic amplitude compared to the conventional method using the modulation of phase opposite disposition. Moreover, the switching count is also decreased by 26.37%.

*Keywords-cascaded multilevel inverter; phase opposite disposition; switching count; total harmonic distortion; individual harmonic*

## I. INTRODUCTION

The growing popularity of renewable energy stems from their environmentally friendly attributes and increasing cost competitiveness [1]. Wind turbines and photovoltaic (PV) panels now play a key role in addressing climate change, reducing pollution and ensuring long-term energy sustainability [2]. However, the power of these sources depends heavily on weather conditions. To serve as an efficient power source, seamless integration into the grid is important, achieved through inverters [3]. Multilevel inverters offer many benefits, including reduced Total Harmonic Distortion (THD), increased voltage and power, and improved efficiency. In general, these advantages enhance the overall performance of the system [4, 5]. These inverters find application in renewable energy systems, high voltage transmission, motor drives and electric vehicles, effectively addressing complex energy conversion needs. Multilevel inverters, which are especially popular, play an important role in grid-connected energy systems by efficiently converting dc sources into ac sources compatible with the power grid. Their popular adoption is due to their ability to integrate smoothly into the grid, enhancing energy output, and promoting sustainable electricity production [6-8]. Because the demand for energy-saving and environmentally friendly solutions is increasing, their popularity is expected to continue to expand [6, 7, 9-12]. However, the power quality of multilevel inverters depends much on the modulation technique. In particular, significant Common Mode Voltage (CMV) magnitude has a detrimental impact on the power

quality of grid-connected inverter systems, leading to the generation of grid leakage currents and harmonics [13]. Several methods are available for modulating multilevel inverters, with the main options being the Sinusoidal Pulse Width Modulation (SPWM) and the space vector modulation [14-17]. SPWM is more efficient as the number of levels increases. Different techniques include Phase Disposition (PD), Phase Opposite Disposition (POD), and Alternating Phase Opposite Disposition (APOD) [18-20], each with its advantages and disadvantages. However, the POD exhibits the ability to generate a CMV magnitude lower than that of the PD. The POD technique is more widely applied due to its simplicity and efficiency. However, this method usually uses a carrier wave with a fixed frequency for modulation. Thus, these carriers do not contain any information about the control signal. On the contrary, in the field of telecommunications, there are many modulation methods that rely on the information of control signals to create carriers, such as amplitude modulation, frequency modulation, phase modulation, and phase shift keying technique. However, in the field of grid-connected multilevel inverters, these techniques have not been applied effectively. Techniques of frequency modulation, e.g. phase modulation in [21], and phase shift keying in [22], have been shown to be effective in multilevel inverter modulation with fixed R-L load. They have the ability to reduce common mode voltage and reduce harmonics effectively similar to that of the POD and APOD methods. However, in the field of grid-connected multi-level inverters, these methods have hardly been applied effectively. Meanwhile, the control quality of

grid-connected inverters depends heavily on the current controllers, phase locking loops and the variation of reference power transmitted to the grid of the inverter system.

This article proposes a technique that combines frequency modulation and phase shift keying for grid-connected multilevel inverter systems. The proposed method's effectiveness in spreading the spectrum over a wide range has resulted in a significant reduction in the peak individual harmonic amplitude. This will help reduce noise in telecommunications and military equipment. The current THD and switching count of the proposed method are also significantly reduced in comparison with those of the POD modulation method.

II. GRID-CONNECTED INVERTER SYSTEM

In Figure 1, a 7-level 3-phase inverter system connected to the grid is shown. The system employs the POD modulation with the fixed carriers, reference current calculation, a current controller, and a Phase-Locked Loop (PLL) for control. Employing the current control method in the Synchronous Rotating Frame (SRF), quantities like  $I_d$ ,  $I_q$ ,  $V_d$ , and  $V_q$  are transformed from the three-phase frame using the phase angle ( $\theta$ ) estimated by the PLL. Subsequently, the reference currents injected into the grid in the SRF, namely  $I_{d-ref}$  and  $I_{q-ref}$ , are calculated according to (1) based on reference powers,  $P_{ref}$  and  $Q_{ref}$ .

$$\begin{bmatrix} I_{d-ref} \\ I_{q-ref} \end{bmatrix} = \frac{(2/3)}{V_d^2 + V_q^2} \begin{bmatrix} V_d & -V_q \\ V_q & V_d \end{bmatrix} \begin{bmatrix} P_{ref} \\ Q_{ref} \end{bmatrix} \quad (1)$$

Based on the error between the reference currents and the actual measurements, the PI controllers fine-tune the reference voltages, specifically  $V_{d-ref}$  and  $V_{q-ref}$ . These voltage values are then transformed into their corresponding reference phase voltages, denoted as  $V_{ref-abc}$ . The POD modulation method uses these phase voltages as inputs, generating pulse signals for switches.

$$G(t) = (V_{ref-abc} + 1) \frac{n-1}{2} \quad (2)$$

$$L_x = \begin{cases} n-2 & \text{if } G(t) \geq n-2 \\ fix(G(t)), & \text{otherwise} \end{cases} \quad (3)$$

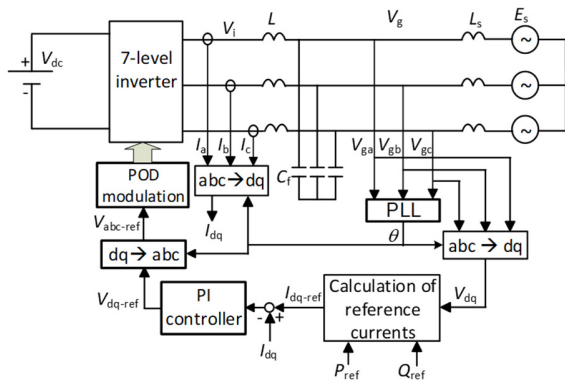


Fig. 1. The grid-connected multilevel inverter system.

The main circuit for one phase shown in Figure 2 displays featuring 3 H-bridges utilizing IGBTs. Each arm of this configuration comprises an upper switch,  $S_{xj1}$ , and a lower switch,  $S_{xj2}$  (where x represents the phases a, b, or c and j ranges from 1 to 6). The output voltage for each phase is detailed in Table I, encompassing seven distinct levels. These voltage levels are contingent upon the outputs  $S_{xj}$  as indicated in the control principle illustrated in Figure 3. This control method is also used and detailed in [21, 23].

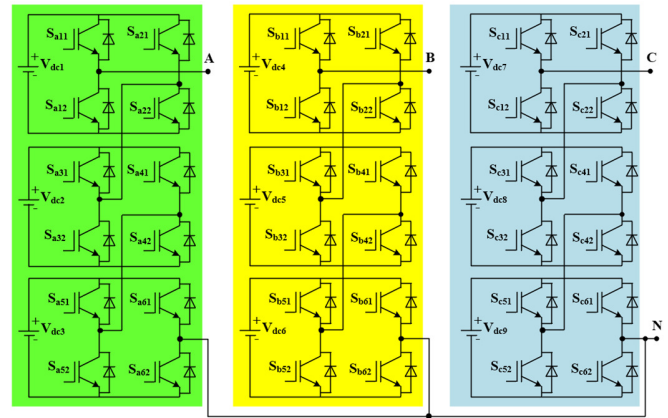


Fig. 2. Main circuit of cascaded 7-level 3-phase inverter.

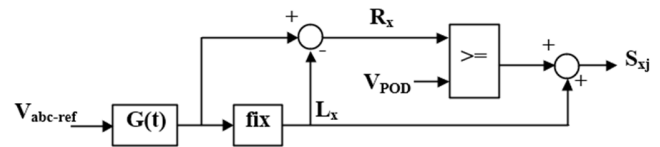


Fig. 3. Control principle of the inverter.

TABLE I. SWITCHING STATES OF SWITCHES OF PHASE A

n	S <sub>a11</sub>	S <sub>a21</sub>	S <sub>a31</sub>	S <sub>a41</sub>	S <sub>a51</sub>	S <sub>a61</sub>	Output Voltage
1	0	1	0	1	0	1	-3V <sub>dc</sub>
2	0	1	0	1	0	0	-2V <sub>dc</sub>
3	0	1	0	0	0	0	-V <sub>dc</sub>
4	0	0	0	0	0	0	0
5	1	0	0	0	0	0	+V <sub>dc</sub>
6	1	0	1	0	0	0	+2V <sub>dc</sub>
7	1	0	1	0	1	0	+3V <sub>dc</sub>

III. THE PROPOSED METHOD

The structure of the proposed method is shown in Figure 4. The proposed modulation is based on the following analysis. In the POD modulation method using carriers with the fixed frequency and phase of a 7-level inverter, the waveforms of phase voltage and current in Figure 5(a) show that the current ripples significantly increase near the peak of the sinusoidal signal. In addition, the spectrum is difficult to spread over a wide range when using the fixed frequency carriers, because the spectra focus on the multiple switching frequency (Figure 5(b)). This leads to increasing the highest individual harmonic magnitude [21, 23]. Moreover, the rms value of current THD is minimum when the current ripples are uniform throughout the

sinusoidal period [24]. Therefore, the carriers need to be modulated for the current ripples equally throughout the period.

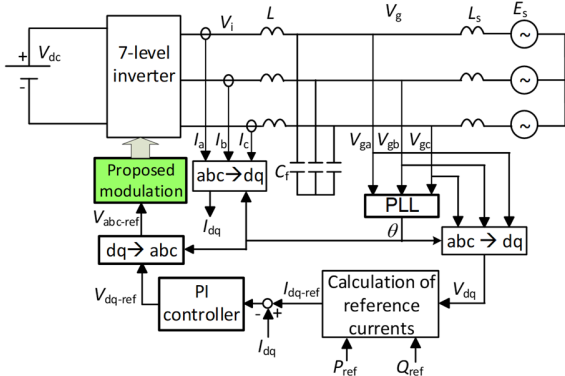


Fig. 4. The proposed method.

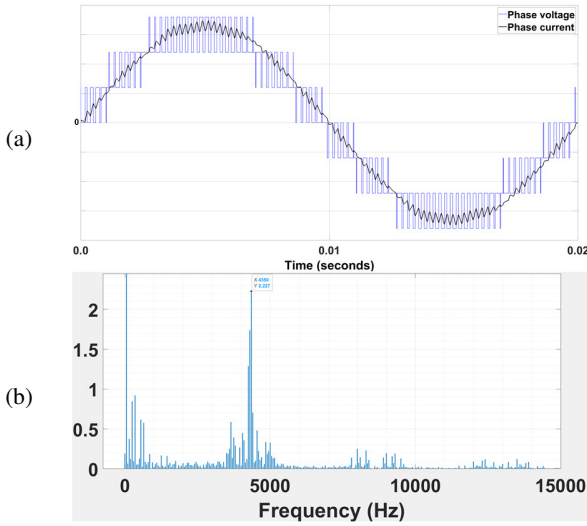


Fig. 5. Seven-level inverter using POD method: (a) Phase voltage and current waveforms, (b) spectrum of phase current for carrier frequency of 4.32 kHz.

A carrier with an amplitude  $V_m$  can be described as:

$$v(t) = V_m \cos(\omega t + \theta) \quad (4)$$

The carrier with fixed frequency used for the POD method before normalization has a form as (5), where  $\omega$  is  $2\pi f$  and  $\theta$  is the phase angle.

$$v_{pod}(t) = \frac{2}{\pi} \sin^{-1}(v(t)) = \frac{2}{\pi} \sin^{-1}(V_m \cos(\omega t + \theta)) \quad (5)$$

The control signal has a sinusoidal form and is described as follows.

$$v_{ref}(t) = V_{max} \sin(\omega t) \quad (6)$$

where  $V_{max}$  is the magnitude of the control signal.

Using the control signal  $v_{ref}(t)$  to vary the frequency of the carrier  $v(t)$  helps obtain the frequency modulated carriers. Then:

$$v_{MC}(t) = V_m \cos[v_{norm}(t) * \omega_c t + \theta] \quad (7)$$

where  $v_{norm}(t)$  is a normal signal, defined as:

$$v_{norm}(t) = \left( |v_{ref}(t)|_{L_y} - C_p \right) m_f + 1 \quad (8)$$

where  $L_y$ ,  $m_f$ , and  $C_p$  represent the optional levels, frequency modulation index, and period index, respectively. Then, we can obtain the carrier after modulation as follows:

$$c_M(t) = \frac{2}{\pi} \sin^{-1}(v_{MC}(t)) \quad (9)$$

Then, using the phase shift keying technique of [22], we can obtain the result as follows:

$$c_m(t) = s(t) * c_M(t) \quad (10)$$

with:

$$s(t) = \begin{cases} +1 & \text{if } v_{ref}(t) \geq 0 \\ -1 & \text{if } v_{ref}(t) < 0 \end{cases} \quad (11)$$

The carrier after normalization becomes:

$$V_M(t) = \frac{\max(c_m(t)) + c_m(t)}{\max(c_m(t)) + \min(c_m(t))} \quad (12)$$

The structure of the proposed method using the modulated carrier is shown in Figure 6. The quantities  $F_L$ ,  $R_x$ , and  $R_0$  are detailed in [23].

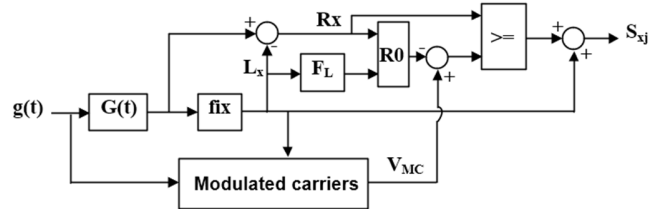


Fig. 6. The proposed control technique using the phase modulated carriers.

#### IV. RESULTS AND DISCUSSION

The system parameters are presented in Table II. There are three intervals of time surveyed in this system. The time of each interval is 0.3 s. In the first interval, 0-0.3 s, the reference active power  $P_{ref}$  is 20 kW and the reference reactive power  $Q_{ref}$  is 0.0 Var. In the second interval, 0.3-0.6 s,  $P_{ref}$  is stepped down to 10 kW while  $Q_{ref}$  is still 0.0 Var. In the third interval, 0.6-0.9 s,  $P_{ref}$  is still 10 kW while  $Q_{ref}$  is stepped from 0.0 Var up to 10 kVar.

The simulation results of the two methods, based on a 7-level 3-phase inverter system, are shown in Figures 7-14. The waveforms of phase voltage A, phase current A, line-line voltage,  $V_{ab}$ , common mode voltage, and carriers for the POD

method can be seen in Figure 8. The phase current waveform in Figure 8(c) is multiplied by 7.7 to get a shape similar to the shape of voltage to easily evaluate the current ripples.

TABLE II. SYSTEM PARAMETERS

Parameter	Symbol	Value
Grid source voltage	$V_g$	3*380 VAC
Grid source frequency	$f_l$	50 Hz
Resistor of the grid source	$R_s$	0.01 $\Omega$
Inductor of the grid source	$L_s$	0.02 mH
Inductor of filter	$L_f$	1.5 mH
Resistor of $L_f$	$R$	0.01 $\Omega$
Capacitor of filter	$C_f$	1 mF
DC voltage	$V_{dc}$	120 V
Coefficients of current controller	$K_p; K_i$	0.15; 20
Frequency of carrier wave in POD	$f_{car}$	4.32 kHz
Center frequency	$f_c$	2.8 kHz
Frequency index	$m_f$	8
Optional levels	$L_n$	0; 5
Period index	$C_p$	2/3

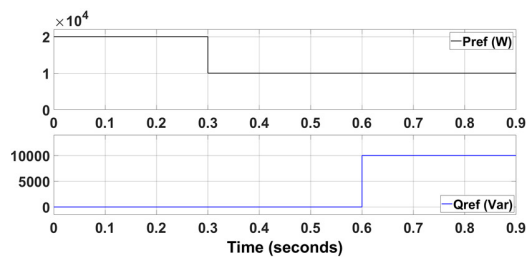


Fig. 7. Waveforms of reference active and reactive powers.

Similarly, the values of the proposed method are shown in Figure 9. The waveforms in Figure 8(c) show that the phase current contains the higher ripples near the peak of the sinusoidal signal. In addition, the switching count in a fundamental period of the phase voltage is up to 182. The CMV magnitude in Figure 8(d) is  $V_{dc}/3$ , the same as that of the proposed method in Figure 9(d).

On the contrary, the phase current waveform of the proposed method shows smoothness in Figure 9(c) compared to that of the POD method in Figure 8(c). The current ripples of the proposed method are evenly distributed throughout the fundamental period due to the modulated carriers in Figure 9(e). Moreover, the switching count of the phase voltage in Figure 9(c) is only 134, lower than the 182 of Figure 8(c). Thus, the switching count of the proposed method is reduced by 26.37% compared to that of the POD method.

The 3-phase current waveforms in Figures 10-11 also show the smoothness of the proposed method. The power ripples of the current injected into the grid by the proposed method are lower than those of the POD method (Figure 12). The switching count of the two methods surveyed in 45 fundamental periods is shown in Figure 13. This shows the ability to effectively reduce the switching count of the proposed method in different operation modes of grid-connected inverters.

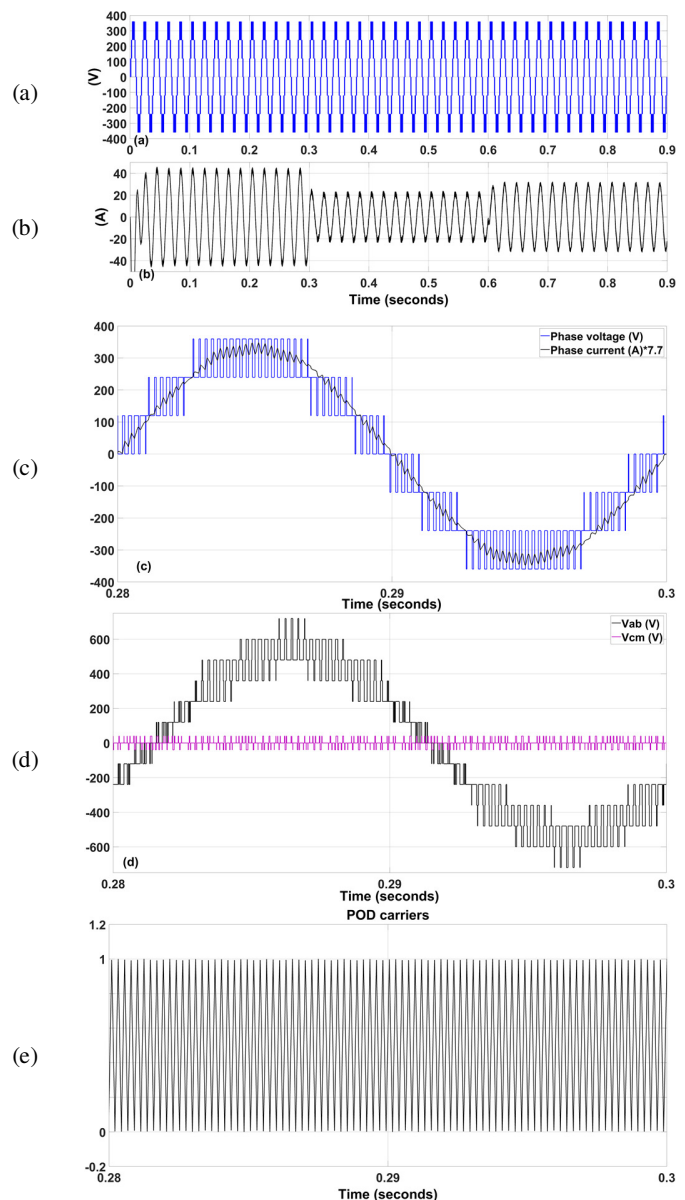
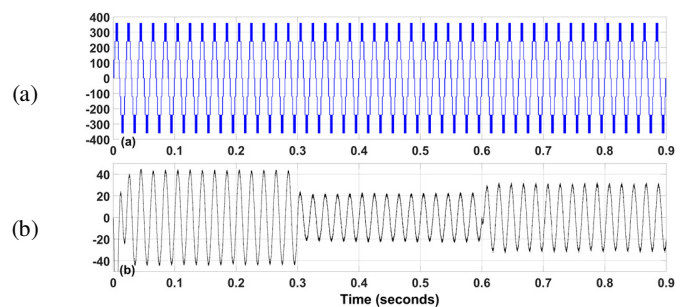


Fig. 8. Phase A waveforms of the POD method taken at the inverter output and before the LC filter. (a) Phase voltage, (b) phase current, (c) voltage and current waveforms zoomed in 0.28-0.3 s, (d) line-to-line voltage and common mode voltage zoomed in 0.28-0.3 s, (e) fixed carriers zoomed in 0.28-0.3 s.



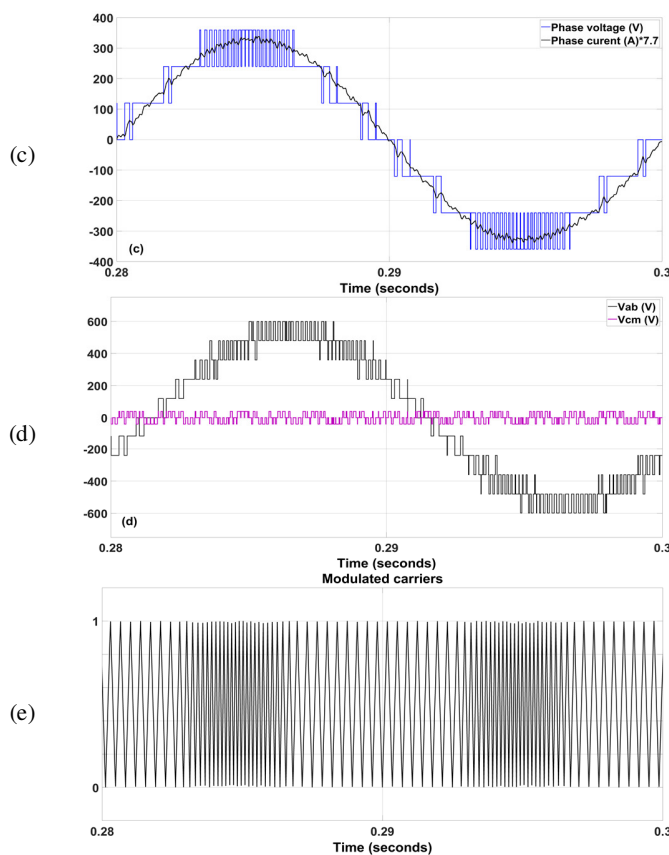


Fig. 9. Phase A waveforms of the proposed method taken at the inverter output and before the LC filter. (a) Phase voltage, (b) phase current, (c) voltage and current waveforms zoomed in 0.28-0.3 s, (d) line-to-line voltage and common mode voltage zoomed in 0.28-0.3 s, (e) fixed carriers zoomed in 0.28-0.3 s.

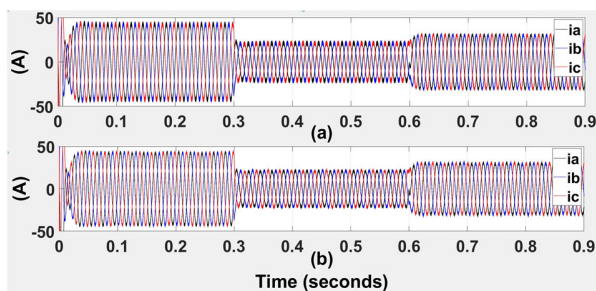


Fig. 10. Three-phase current waveforms injected into the grid. (a) POD method, (b) proposed method.

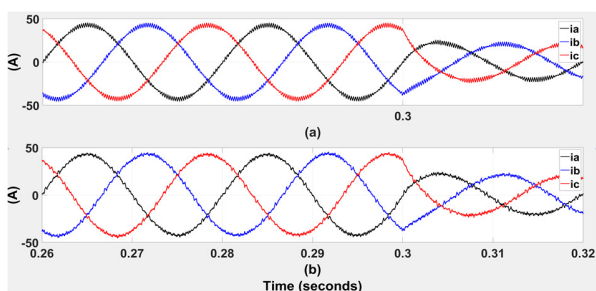


Fig. 11. Three-phase current waveforms injected into the grid zoomed in 0.26-0.32 s. (a) POD method, (b) proposed method.

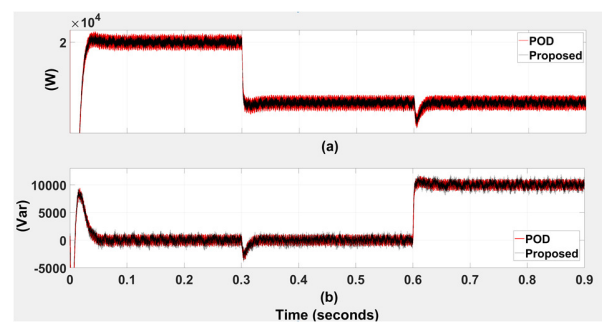


Fig. 12. Powers injected into the grid. (a) Active powers, (b) reactive powers.

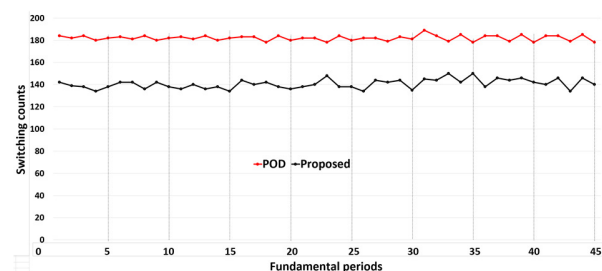


Fig. 13. Switching count in fundamental periods.

Additionally, the ability to reduce the current THD and spread the spectrum over a wide range is shown in Figure 14. The phase current THD values of the POD method in Figures 14(a)-(c) are 3.58%, 7.16%, and 5.03%, respectively. These values are higher than those of the proposed method (3.01%, 5.93%, and 4.13%) as shown in Figures 14(d)-(f). Thus, in the nominal operation, the current THD value of the proposed method in Figure 14(d) is reduced by 15.92% compared to the POD method using the fixed frequency carriers.

Besides, the ability to spread the spectrum of the proposed method reduces the highest individual harmonic magnitude in Figures 14(d)-(f) as 1.0%, 2.3%, and 1.31%, respectively. The spectrum of the POD method focuses on the multiple fixed frequency of carriers. This leads to the highest individual harmonic magnitude in Figures 14(a)-(c) up to 2.136%, 4.31%, and 3%, respectively. Therefore, in the nominal operation, the highest individual harmonic magnitude of the proposed method is reduced by 48.5% compared to that of the POD method using the unmodulated carriers.

## V. CONCLUSION

Although the technique of carrier modulation has been popular in telecommunications, it has not been used in grid-connected inverters. The contribution of this article is the analysis of the effects of the modulation carrier on the power quality of the inverters. Then, a method using the control signal to modulate the frequency of carrier and the technique of phase shift keying to modulate the phase of carrier is proposed. The results of the proposed method are compared with those of the POD method using unmodulated carriers. The ability to spread spectrum over a wide range is one of the advantages of the proposed method.

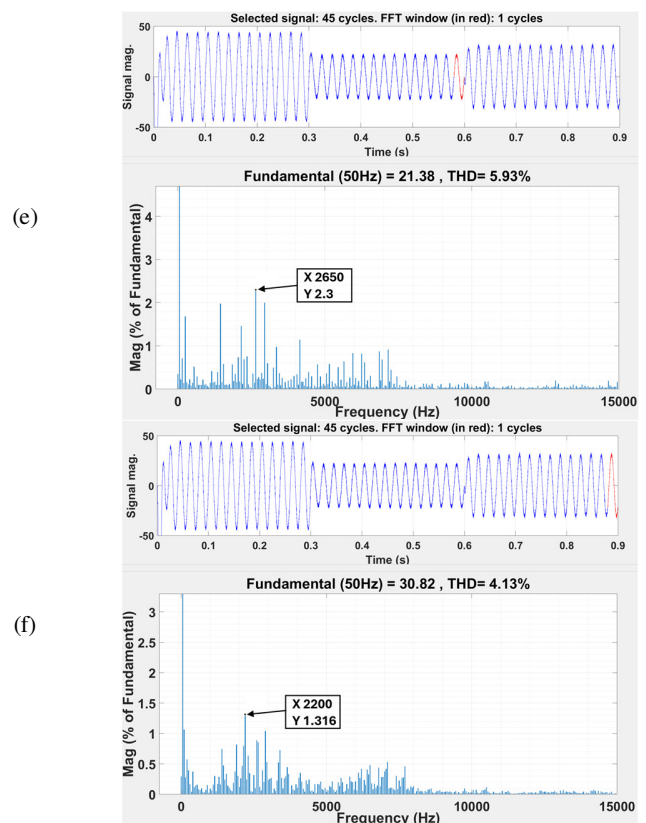
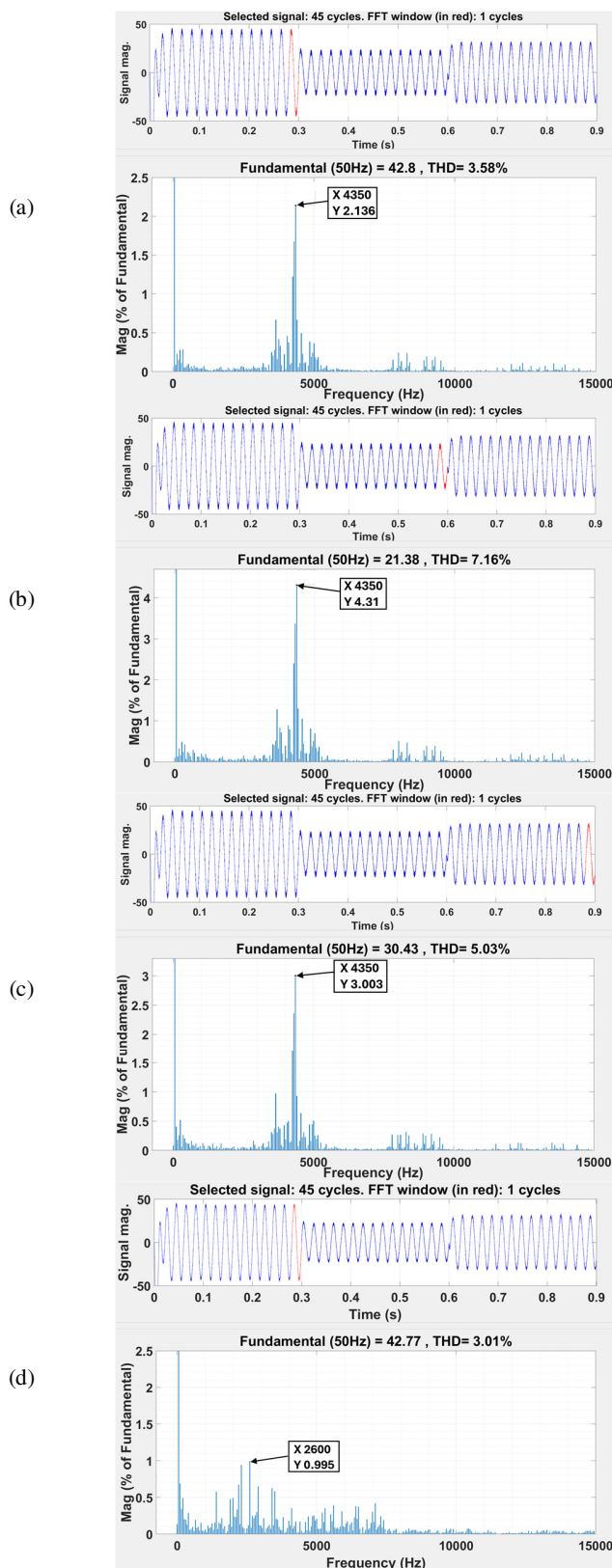


Fig. 14. Spectra and THD of phase current. (a)-(c) POD method. (d)-(f) proposed method.

The simulation results based on the grid-connected system using cascaded 7-level 3-phase inverter have confirmed the effectiveness of the proposed method compared with that of the method using the POD modulation. The CMV, THD values, individual harmonics, and the number of switching counts are considered and evaluated quantitatively. In the nominal operational mode, the proposed method helps to reduce the current THD, the magnitude of the highest individual current harmonic, and the switching count by 15.92%, 48.5%, and 26.37% respectively, compared with those of the POD method.

ACKNOWLEDGMENT

This work belongs to the project in 2024 funded by Ho Chi Minh City University of Technology and Education, Vietnam.

REFERENCES

- [1] Y. Kassem, H. Camur, and E. G. Ghoshouni, "Assessment of a Hybrid (Wind-Solar) System at High-Altitude Agriculture Regions for achieving Sustainable Development Goals," *Engineering, Technology & Applied Science Research*, vol. 14, no. 1, pp. 12595–12607, Feb. 2024, <https://doi.org/10.48084/etasr.6494>.
- [2] X. D. Dam, M. Vu, Q. N. Nguyen, T. T. Huong Nguyen, and X. D. Dam, "Development of renewable energy sources to serve agriculture in Vietnam: SWOT and TOWS analysis based strategy assessment," in *Asia Meeting on Environment and Electrical Engineering*, Hanoi, Vietnam, Nov. 2023, pp. 1–6, <https://doi.org/10.1109/EEE-AM58328.2023.10395652>.
- [3] T. Lachumanan, R. Singh, M. I. Shapiyai, and T. J. S. Anand, "Analysis of a Multilevel Voltage-Based Coordinating Controller for Solar-Wind Energy Generator: A Simulation, Development and Validation

- Approach," *Engineering, Technology & Applied Science Research*, vol. 11, no. 6, pp. 7793–7799, Dec. 2021, <https://doi.org/10.48084/etasr.4489>.
- [4] U. B. Tayab and M. A. A. Humayun, "Modeling and Analysis of a Cascaded Battery-Boost Multilevel Inverter Using Different Switching Angle Arrangement Techniques," *Engineering, Technology & Applied Science Research*, vol. 7, no. 2, pp. 1450–1454, Apr. 2017, <https://doi.org/10.48084/etasr.1094>.
- [5] Y. Gopal, K. P. Panda, D. Birla, and M. Lalwani, "Swarm Optimization-Based Modified Selective Harmonic Elimination PWM Technique Application in Symmetrical H-Bridge Type Multilevel Inverters," *Engineering, Technology & Applied Science Research*, vol. 9, no. 1, pp. 3836–3845, Feb. 2019, <https://doi.org/10.48084/etasr.2397>.
- [6] S. Mehta and V. Puri, "A review of different multi-level inverter topologies for grid integration of solar photovoltaic system," *Renewable Energy Focus*, vol. 43, pp. 263–276, Dec. 2022, <https://doi.org/10.1016/j.ref.2022.10.002>.
- [7] G. Griva, S. Musumeci, R. Bojoi, P. Zito, S. Bifaretti, and A. Lampasi, "Cascaded multilevel inverter for vertical stabilization and radial control power supplies," *Fusion Engineering and Design*, vol. 189, Apr. 2023, Art. no. 113473, <https://doi.org/10.1016/j.fusengdes.2023.113473>.
- [8] A. Mittal, K. Janardhan, and A. Ojha, "Multilevel inverter based Grid Connected Solar Photovoltaic System with Power Flow Control," in *International Conference on Sustainable Energy and Future Electric Transportation*, Hyderabad, India, Jan. 2021, pp. 1–6, <https://doi.org/10.1109/SeFet48154.2021.9375753>.
- [9] W. Rahmouni, G. Bachir, and M. Aillerie, "A new control strategy for harmonic reduction in photovoltaic inverters inspired by the autonomous nervous system," *Journal of Electrical Engineering*, vol. 73, no. 5, pp. 310–317, Sep. 2022, <https://doi.org/10.2478/jee-2022-0041>.
- [10] N. T. Mbungu, R. M. Naidoo, R. C. Bansal, M. W. Siti, and D. H. Tungadio, "An overview of renewable energy resources and grid integration for commercial building applications," *Journal of Energy Storage*, vol. 29, Jun. 2020, Art. no. 101385, <https://doi.org/10.1016/j.est.2020.101385>.
- [11] J. Stottner, A. Rauscher, and C. Endisch, "Pareto optimization of multilevel inverter structures regarding the DC magnitude, switching frequency and switching angles," *International Journal of Electrical Power & Energy Systems*, vol. 142, Nov. 2022, Art. no. 108259, <https://doi.org/10.1016/j.ijepes.2022.108259>.
- [12] C. Dhanamjayulu, P. Sanjeevikumar, and S. M. Muyeen, "A structural overview on transformer and transformer-less multi level inverters for renewable energy applications," *Energy Reports*, vol. 8, pp. 10299–10333, Nov. 2022, <https://doi.org/10.1016/j.egyr.2022.07.166>.
- [13] C.-C. Hou, C.-C. Shih, P.-T. Cheng, and A. M. Hava, "Common-Mode Voltage Reduction Pulsewidth Modulation Techniques for Three-Phase Grid-Connected Converters," *IEEE Transactions on Power Electronics*, vol. 28, no. 4, pp. 1971–1979, Apr. 2013, <https://doi.org/10.1109/TPEL.2012.2196712>.
- [14] E. Babaei and S. Laali, "A Multilevel Inverter with Reduced Power Switches," *Arabian Journal for Science and Engineering*, vol. 41, no. 9, pp. 3605–3617, Sep. 2016, <https://doi.org/10.1007/s13369-016-2217-0>.
- [15] H. K. Busireddy, M. M. Lokhande, R. R. Karasani, and V. B. Borghate, "A Modified Space Vector PWM Approach for Nine-Level Cascaded H-Bridge Inverter," *Arabian Journal for Science and Engineering*, vol. 44, no. 3, pp. 2131–2149, Mar. 2019, <https://doi.org/10.1007/s13369-018-3363-3>.
- [16] W. Li, X. Zhang, Z. Zhao, G. Zhang, G. Wang, and D. Xu, "Implementation of Five-Level DPWM on Parallel Three-Level Inverters to Reduce Common-Mode Voltage and AC Current Ripples," *IEEE Transactions on Industry Applications*, vol. 56, no. 4, pp. 4017–4027, Jul. 2020, <https://doi.org/10.1109/TIA.2020.2991020>.
- [17] T. Liu, A. Chen, C. Qin, J. Chen, and X. Li, "Double Vector Model Predictive Control to Reduce Common-Mode Voltage Without Weighting Factors for Three-Level Inverters," *IEEE Transactions on Industrial Electronics*, vol. 67, no. 10, pp. 8980–8990, Oct. 2020, <https://doi.org/10.1109/TIE.2020.2994876>.
- [18] M. Jamil, "Carrier-based modulation strategies for a neutral point clamped inverter," *International Journal of Electronics*, vol. 95, no. 12, pp. 1293–1303, Jan. 2008, <https://doi.org/10.1080/00207210802524294>.
- [19] A. Alexander Stonier, "Design and development of high performance solar photovoltaic inverter with advanced modulation techniques to improve power quality," *International Journal of Electronics*, vol. 104, no. 2, pp. 174–189, Feb. 2017, <https://doi.org/10.1080/00207217.2016.1196746>.
- [20] P. S. Kumar and M. Satyanarayana, "Comparative analysis of modulation strategies applied to seven-level diode clamped multi-level inverter fed induction motor drive," in *Conference on Power, Control, Communication and Computational Technologies for Sustainable Growth*, Kurnool, India, Dec. 2015, pp. 231–237, <https://doi.org/10.1109/PCCTSG.2015.7503893>.
- [21] V.-Q. Nguyen and Q.-T. Tran, "Common mode voltage reduction of cascaded multilevel inverters using carrier frequency modulation," *International Journal of Electronics*, vol. 109, no. 8, pp. 1324–1351, Aug. 2022, <https://doi.org/10.1080/00207217.2021.1969437>.
- [22] V.-Q. Nguyen and Q. Tran, "Reduction of common mode voltage for cascaded multilevel inverters using phase shift keying technique," *Indonesian Journal of Electrical Engineering and Computer Science*, vol. 21, no. 2, pp. 691–706, Feb. 2021, <https://doi.org/10.11591/ijeeecs.v21.i2.pp691-706>.
- [23] Q.-T. Tran and V.-Q. Nguyen, "Reduction of common mode voltage for grid-connected multilevel inverters using fuzzy logic controller," *International Journal of Power Electronics and Drive Systems*, vol. 14, no. 2, pp. 698–707, Jun. 2023, <https://doi.org/10.11591/ijpedes.v14.i2.pp698-707>.
- [24] Q.-T. Tran, A. V. Truong, and P. M. Le, "Reduction of harmonics in grid-connected inverters using variable switching frequency," *International Journal of Electrical Power & Energy Systems*, vol. 82, pp. 242–251, Nov. 2016, <https://doi.org/10.1016/j.ijepes.2016.03.027>.